Optics Letters

Slow-light effect via Rayleigh anomaly and the effect of finite gratings

Kyoung-Youm Kim,[1,2] Xinyuan Chong,[1] Fanghui Ren,[1] and Alan X. Wang[1,*]

[1]School of Electrical Engineering and Computer Science, Oregon State University, Corvallis, Oregon 97331, USA
[2]Department of Electrical Engineering, Sejong University, Seoul 05006, South Korea
*Corresponding author: wang@eecs.oregonstate.edu

Received 16 September 2015; revised 17 October 2015; accepted 19 October 2015; posted 19 October 2015 (Doc. ID 250230); published 10 November 2015

In this Letter, we investigate the slow-light effect of subwavelength diffraction gratings via the Rayleigh anomaly using a fully analytical approach without needing to consider specific grating structures. Our results show that the local group velocity of the transmitted light can be significantly reduced due to the optical vortex, which can inspire a new mechanism to enhance light–matter interactions for optical sensing and photodetection. However, the slow-light effect will diminish as the transmitted light propagates farther from the grating surface, and the slowdown factor decreases as the grating size shrinks.

OCIS codes: (050.1950) Diffraction gratings; (050.6624) Subwavelength structures; (260.2110) Electromagnetic optics.

http://dx.doi.org/10.1364/OL.40.005339

Diffraction gratings change the direction of incoming light [1]. The Rayleigh anomaly (sometimes called the Wood or Rayleigh–Wood anomaly) indicates the phenomenon when diffracted lights are directed perpendicular to the surface normal of the grating [2–4]. Recently, it has attracted strong research interest due to its interplay with surface plasmon polariton (SPP) waves [5–13]. Applications such as extraordinary transmission (EOT) [11] and high-sensitivity optical sensors [9] have already been proposed and demonstrated. The interaction between SPP waves and the Rayleigh anomaly will result in a highly localized optical field that is determined by the decaying SPP waves, typically on the order of one wavelength. Interestingly, people find that Rayleigh anomaly alone can exhibit unique characteristics that are distinctively different from SPP waves. In this Letter, we explicitly point out that the Rayleigh anomaly can slow down the group velocity of the transmitted light, similar to the effect from photonic crystal waveguides [14] and plasmonic waveguide gratings [15]. More importantly, this slow light effect can extend much farther from the grating surface than the SPP waves. This can increase the interaction time between light and matter over a long path, which contrasts with conventional plasmonic biosensing relying on nano-scale hot-spots [16], and the comparison has been discussed in [17,18]. Therefore, the slow light effect of RA can be applied to the realization of enhanced optical sensing (especially infrared absorption of gases) and photon detection close to the bandgap of semiconductors. However, we found that both the slowdown factor and the effective range depend on the grating size. Therefore, we further investigate the finite-size effect of gratings that is unavoidable in actual applications.

We begin our discussion with the grating shown in Fig. 1(a). It has a period L_g and can be made of dielectrics or metals. If it is metallic, we assume further that it is not thick enough for the perforations between metallic grooves to guide SPP waves along the z direction. Since our target applications are sensors utilizing the enhanced interaction between slow light and objects in free space, we limit our attention to the transmission-type grating. A TM-polarized light, propagating in the $+z$ direction, is assumed to be normally incident to this grating. Since the grating is periodic infinitely, the magnetic field distribution at its exit plane (taken as $z = 0$) can be expanded as

$$\mathbf{H}_I(x, 0) = \hat{\mathbf{y}} \sum_{n=-\infty}^{\infty} a_n e^{jn\Lambda x}, \tag{1}$$

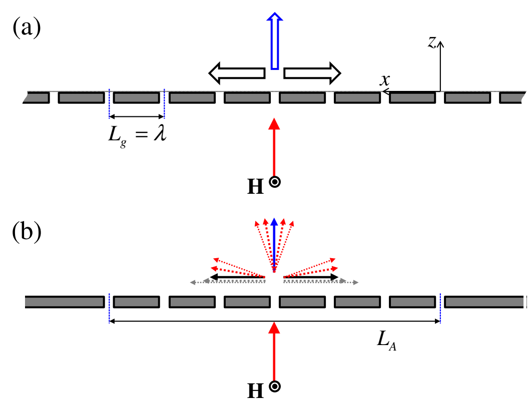

Fig. 1. Geometry of the (a) infinite and (b) finite gratings. In (a), the transmitted light has only three wave vectors (see the blue and black unfilled arrows). However, the finite-size effect induces additional wave vectors around each of them [see the dotted red and gray arrows in (b) that correspond to the propagating and evanescent diffracted waves, respectively].

where $\Lambda = 2\pi/L_g$. a_n represents the amplitude of the n-th harmonic field component that can be easily obtained by either the finite element method (FEM) or the rigorous coupled wave analysis (RCWA).

Using the angular spectrum expansion [1], the magnetic field of the transmitted light in $z>0$ can be written as

$$\mathbf{H}_I = \hat{\mathbf{y}} \sum_{n=-\infty}^{\infty} a_n e^{j\left(n\Lambda x + \sqrt{k_0^2-(n\Lambda)^2}z\right)}, \tag{2}$$

where $k_0 = 2\pi/\lambda$ and λ is the wavelength of light in free space. The Rayleigh anomaly occurs when $L_g \approx \lambda$, resulting in [19]

$$\mathbf{H}_I = \hat{\mathbf{y}}[a_0 e^{jk_0 z} + 2a_1 \cos(k_0 x)], \tag{3}$$

where we considered only the first-order diffraction. For the simplicity of discussion, we also assumed that the grating structure (e.g., its permittivity distribution) is symmetric with respect to the z axis, which makes a_1 real.

Using Eq. (3), we can easily derive

$$\tilde{S}_x = 2|a_0 a_1| \sin(k_0 x) \sin(k_0 z + \angle a_0 a_1), \tag{4}$$

$$\tilde{S}_z = |a_0|^2 + 2|a_0 a_1| \cos(k_0 x) \cos(k_0 z + \angle a_0 a_1), \tag{5}$$

$$\tilde{w} = |a_0|^2 + 2|a_1|^2 + 2|a_0 a_1| \cos(k_0 x) \cos(k_0 z + \angle a_0 a_1), \tag{6}$$

where $\mathbf{S} = (\eta_0/2)(\tilde{S}_x, \tilde{S}_z)$ and $w = (\mu_0/2)\tilde{w}$ denote the Poynting vector and energy density of the transmitted light, respectively. η_0 and μ_0 are the impedance and permeability of free space, and their quotient becomes the speed of light in free space ($c = \eta_0/\mu_0$). The energy velocity of light can be obtained by $\mathbf{v} = \mathbf{S}/w$ [20], resulting in

$$v_z(x, z > 0) = c\left(1 - \frac{2|a_1|^2}{\tilde{w}}\right). \tag{7}$$

It is well known that this velocity coincides with the group velocity of light in free space [21–23]. Equation (7) shows that the amount of velocity reduction is determined by how much energy of the transmitted light is stored purely in the diffracted-wave components.

One more phenomenon to note is the so-called optical vortex [19,24–26]. Equations (4) and (5) show that the Poynting vector becomes zero at the points whose coordinates satisfy

$$2\cos(k_0 x)\cos(k_0 z + \angle a_0 a_1) = -|a_0|/|a_1|, \tag{8}$$

$$\sin(k_0 x)\sin(k_0 z + \angle a_0 a_1) = 0. \tag{9}$$

Because optical power cannot flow through these points, optical vortices appear as a kind of detour around them. They increase the effective path length of the transmitted light and effectively reduce its velocity in the longitudinal direction. It is notable that such singular points and resultant vortices can appear only when $\eta = |a_1|/|a_0| \geq 0.5$ [see Eq. (8)].

In Figs. 2(a) and 2(b), we plotted the longitudinal velocity v_z of the transmitted light at $x = 0$, taking different values of η^2. They show clearly that the larger η^2 is, the slower the spatial average of v_z tends to be. Moreover, the vortex effect becomes effective when $\eta^2 \geq 0.25$, resulting in negative v_z [see Fig. 2(c) for an exemplary distribution of Poynting vectors when such vortices are formed through a metallic grating]. This can significantly slow down the average group velocity of the transmitted light. We note that the transverse velocity v_x is zero at $x = m\ (\lambda/2)$ [where m is an integer; see Eq. (4)]. This is because the grating generates two counter-propagating lights that can produce standing waves in the transverse direction. These characteristics reveal that the Rayleigh anomaly can

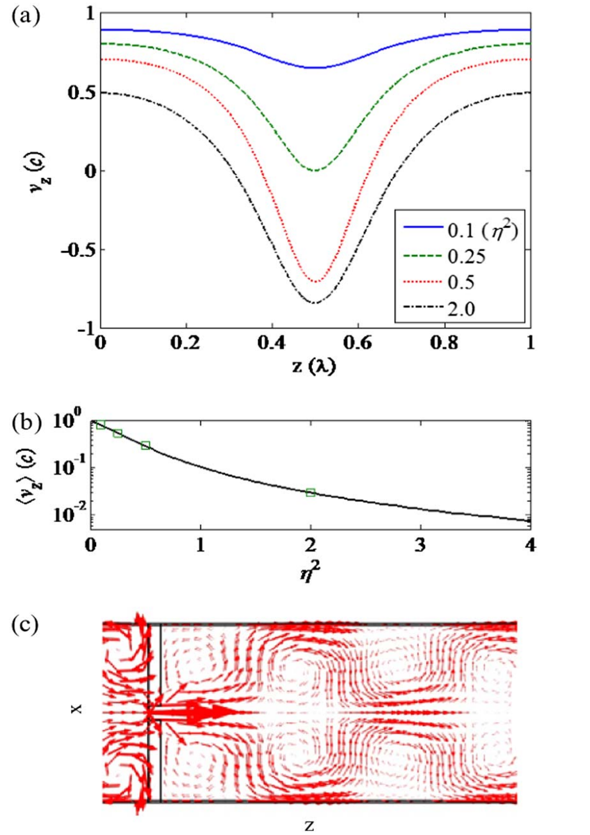

Fig. 2. (a) Longitudinal velocity (v_z) of the transmitted light at $x = 0$. Since the grating is assumed to be infinite, v_z becomes periodic in the z direction. (b) Spatial average of v_z ($\langle v_z \rangle$) over one wavelength along the z direction. (c) Exemplary distribution of Poynting vectors, exhibiting optical vortices.

be used to slow down light in free space. Ideally, the optical field pattern of the transmitted light will repeat itself with period of λ along the z direction, which indicates an infinitely long effective range for slow light.

However, in actual applications, the grating size is always finite, but to take this "finiteness" into account is quite troublesome. If we use RCWA methods, we always come to impose a periodicity on the grating. FEM calculations can be useful but, if the grating size is quite large (but finite), heavy computer resources and high calculation times are required. There are a few semi-analytical methods that basically treat the finite grating as an array of electromagnetic radiators or scatters [27,28]. However, they are somewhat too complicated and are not adequate for gratings with more than $\sim 10^3$ periods. Hereafter, we will develop a simple way of dealing with finite gratings, and investigate how their "finiteness" effects on the slowdown factor and slow light effective range via the Rayleigh anomaly.

Let us look at Fig. 1(b) where we depicted a finite size grating with a length of L_A. In this case, the magnetic field distribution at the exit plane will be no longer periodic. Therefore, instead of Eq. (1), we have

$$\mathbf{H}_F(x, 0) = \hat{\mathbf{y}} \frac{1}{2\pi} \int T(k_x) e^{jk_x x} \mathrm{d}k_x, \tag{10}$$

where $T(k_x)$ is the Fourier transform (FT) of $\mathbf{H}_F(x, 0) \cdot \hat{\mathbf{y}}$. Since we can presume $\mathbf{H}_F(x, 0) \cdot \hat{\mathbf{y}} = (\mathbf{H}_I(x, 0) \cdot \hat{\mathbf{y}})\mathrm{rect}(x/L_A)$,

$T(k_x)$ can be calculated by the convolution of the FT of $\mathbf{H}_I(x,0)\cdot\hat{\mathbf{y}}$ and that of $\mathrm{rect}(x/L_A)$, i.e., $L_A\mathrm{sinc}(L_A k_x/2\pi)$. Using Eq. (1), we can write the FT of $\mathbf{H}_I(x,0)\cdot\hat{\mathbf{y}}$ as $2\pi\sum_n a_n\delta(k_x-n\Lambda)$, which entails

$$T(k_x)=L_A\sum_n a_n\,\mathrm{sinc}\left(\frac{L_A(k_x-nk_0)}{2\pi}\right). \tag{11}$$

To take only the first-order diffraction into account, we need to consider just three terms of this summation corresponding to $n=-1$ to 1. Then, we have

$$\begin{aligned}\mathbf{H}_F=\hat{\mathbf{y}}\frac{L_A}{2\pi}\Bigg[&a_0\int\mathrm{sinc}\left(\frac{L_Ak_x}{2\pi}\right)e^{jk_xx}e^{j\sqrt{k_0^2-k_x^2}z}\mathrm{d}k_x\\&+a_1\int\mathrm{sinc}\left(\frac{L_Ak_x}{2\pi}\right)e^{j(k_x+k_0)x}e^{j\sqrt{k_0^2-(k_x+k_0)^2}z}\mathrm{d}k_x\\&+a_1\int\mathrm{sinc}\left(\frac{L_Ak_x}{2\pi}\right)e^{j(k_x-k_0)x}e^{j\sqrt{k_0^2-(k_x-k_0)^2}z}\mathrm{d}k_x\Bigg].\end{aligned} \tag{12}$$

We can further approximate Eq. (12) by changing each integral into a summation over an integer n with the substitution of $k_x=(n\Delta)k_0$. Fortunately, we do not need to consider large values of k_x (or $n\Delta$) because the sinc function becomes negligible for them. Let us define $n_{\max}$ as the maximum value of n. Then, the maximum argument of the sinc function becomes $n_{\max}\Delta N_g$ where $N_g=L_A/L_g$ (the number of periods in the finite grating). If we want to take into account up to M side lobes of the sinc function, we can put $n_{\max}\Delta N_g=M$. This entails $n_{\max}\Delta=M/N_g<<1$ since 3 or 4 is enough for M. We can thus use $\sqrt{k_0^2-k_x^2}=k_0\sqrt{1-(n\Delta)^2}\approx k_0$ and $\sqrt{k_0^2-(k_x\mp k_0)^2}\approx k_0\sqrt{\pm 2n\Delta}$.

After some algebra with these approximations,

$$\begin{aligned}\mathbf{H}_F=\hat{\mathbf{y}}\Bigg[&a_0'e^{jk_0z}+2\sum_{n=1}^{n_{\max}}\chi_{0n}\cos(n\Delta k_0x)e^{jk_0z}\\&+2a_1'\cos(k_0x)+2\sum_{\substack{n=-n_{\max}\\n\neq0}}^{n_{\max}}\chi_{1n}\cos[(1-n\Delta)k_0x]e^{j\sqrt{2n\Delta}k_0z}\Bigg],\end{aligned} \tag{13}$$

where $a_{0(1)}'=(\Delta N_g)a_{0(1)}$ and $\chi_{0(1)n}=a_{0(1)}'\mathrm{sinc}(n\Delta N_g)$. Let us compare Eq. (13) with Eq. (3). In the case of an infinite grating, the transmitted light has only three wave vectors: (i) $\mathbf{k}_0[=(0,k_0)=k_0(0,1)]$, (ii) $\mathbf{k}_{+1}[=(k_0,0)=k_0(1,0)]$, and (iii) $\mathbf{k}_{-1}[=(-k_0,0)=k_0(-1,0)]$. However, the "finiteness" of the grating brings forth additional wave vectors *around* each of them as is schematically shown in Fig. 1(b): $\mathbf{k}_0^{(n)}=k_0(n\Delta,1)$ and $\mathbf{k}_{\pm1}^{(n)}=k_0(\pm(1-n\Delta),\sqrt{2n\Delta})$. We should point out that half of $\mathbf{k}_{\pm1}^{(n)}$ (with $n<0$) corresponds to evanescent diffracted waves.

Equation (13) results in

$$v_z(x,z>0)=c\left(1-\frac{2\Theta}{\tilde{w}}\right), \tag{14}$$

where $\Theta=\Theta_{\mathrm{pr}}+\Theta_{\mathrm{ev}}$. Θ_{pr} and Θ_{ev} are related to the amounts of velocity reduction due to the propagating and evanescent diffracted waves, respectively [see the fourth term of the right side of Eq. (13)], and are given by

$$\begin{aligned}\Theta_{\mathrm{pr}}=&|a_1'|^2+\sum_{n>0}|\chi_{1n}|^2+2\sum_{n>0}|a_1'\chi_{1n}|\cos(n\Delta k_0x)\\&\times\cos\left(\sqrt{2n\Delta}k_0z\right)\\&+2\sum_{n>0}\sum_{m>n}|\chi_{1n}\chi_{1m}|\cos[(m-n)\Delta k_0x]\\&\times\cos\left[\left(\sqrt{2n\Delta}-\sqrt{2m\Delta}\right)k_0z\right],\end{aligned} \tag{15}$$

$$\begin{aligned}\Theta_{\mathrm{ev}}=&\sum_{n<0}|\chi_{1n}|^2e^{-2\sqrt{2|n|\Delta}k_0z}+2\sum_{n<0}|a_1'\chi_{1n}|e^{-\sqrt{2|n|\Delta}k_0z}\\&\times\cos(n\Delta k_0x)+2\sum_{n<0}\sum_{\substack{m>n\\m\neq0}}|\chi_{1n}\chi_{1m}|e^{-\left(\sqrt{2|n|\Delta}+\mathrm{Im}\left\{\sqrt{2m\Delta}\right\}\right)k_0z}\\&\times\cos[(m-n)\Delta k_0x]\cos(\sqrt{2m\Delta}k_0z).\end{aligned} \tag{16}$$

The above results show that for our analysis of a finite grating, just the values of a_0 and a_1 that the finite grating would have if its size becomes infinite are required into further details of the grating structure are necessary. This is an advantage in that these results can be applied to a wide range of gratings.

Now, let us observe the finite-size effect numerically. In Figs. 3(a) and 3(b), we compared the longitudinal velocities of the transmitted light through finite gratings of different lengths. We set $x=0$ and assumed the same grating structure so that a_0, a_1, and η remain the same in all cases ($\eta^2=1$). The results show that a smaller N_g makes the vortex effect vanish after some propagation distance [see Fig. 3(a)], as a result of which the spatial average of v_z increases as the transmitted light propagates farther from the grating [see Fig. 3(b)]. To examine this further, we calculated $v_z(0,z)$ with $\Theta=\Theta_{\mathrm{pr}}$ (neglecting Θ_{ev}) and vice versa, and plotted the results in Fig. 3(c) [when $N_g=10^3$]. The figure clearly demonstrates that such waning of

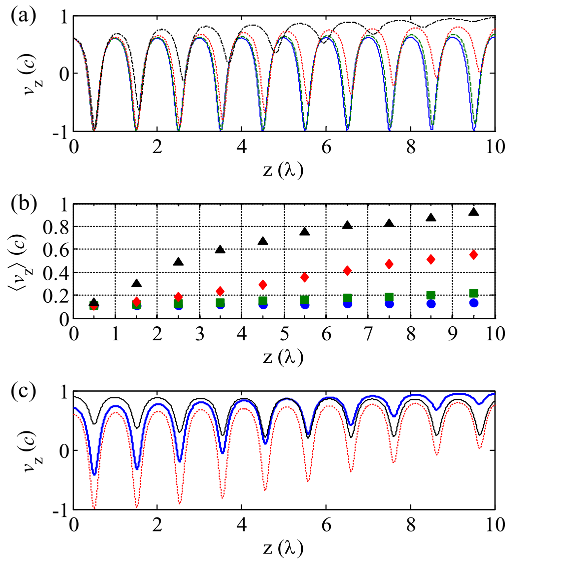

Fig. 3. Finite-size effect of the grating on (a) v_z and (b) $\langle v_z\rangle$ at $x=0$. Solid, dashed, dotted, and dashed-dotted lines in (a) and circles, squares, diamonds, and triangles in (b) correspond to $N_g=10^5$, 10^4, 10^3, and 10^2, respectively. (c) Values of $v_z(0,z)$ with $\Theta=\Theta_{\mathrm{pr}}$ (thin solid) and $\Theta=\Theta_{\mathrm{ev}}$ (thick solid) when $N_g=10^3$. The dotted line corresponds to $\Theta=\Theta_{\mathrm{pr}}+\Theta_{\mathrm{ev}}$ shown in (a).

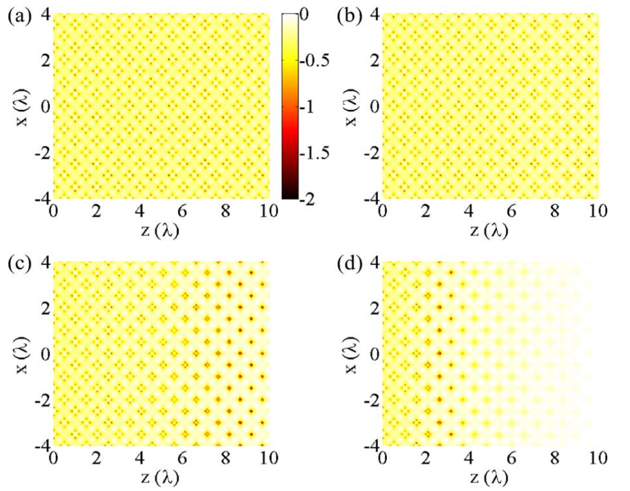

Fig. 4. Finite-size effect of the grating on the speed of the transmitted light, $|\mathbf{v}|(x, z)$. (a)–(d) correspond to the cases of $N_g = 10^5$, 10^4, 10^3, and 10^2, respectively. Note that we have plotted the logarithmic values of the speed, i.e., $\log_{10}(|\mathbf{v}|/c)$, setting its minimum to be −2.

the "slowdown" feature via the Rayleigh anomaly results mostly from Θ_{ev} or the contribution of evanescent diffracted waves.

In contrast to the infinite grating case, the grating geometry is not symmetric with respect to the translation in the x direction. This makes v_x not vanish, even at $x = m(\lambda/2)$ [except for $m = 0$]. We thus showed the logarithmic values of $|\mathbf{v}|$, i.e., the speed of the transmitted light in Fig. 4. The results exhibit that the "slowdown" characteristics via the Rayleigh anomaly can be implemented at not only on-axis, but also off-axis points. In Fig. 5, we further plotted the spatial average values of $|\mathbf{v}|$ at $x = 0.2N_g$ and $0.4N_g$, comparing with those at the on-axis points. It is quite evident from the figures that the variations in the speed of light (along both the x and z directions) become more noticeable when the grating size gets shorter. In many practical

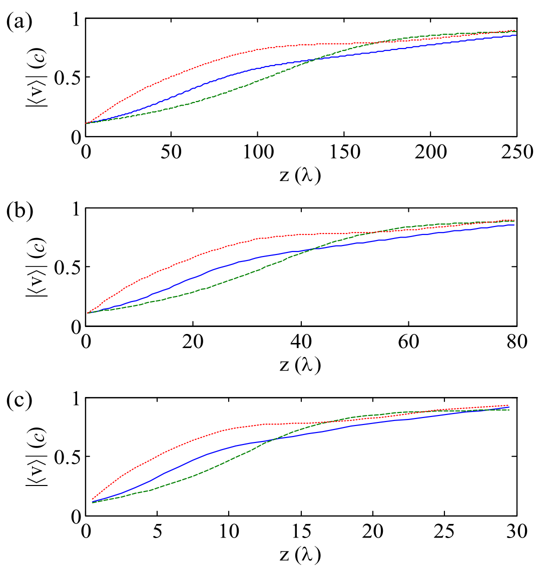

Fig. 5. Spatial average of the speed ($\langle|\mathbf{v}|\rangle$) of the transmitted light when N_g is (a) 10^5, (b) 10^4, and (c) 10^3. Solid, dashed, and dotted lines in each figure correspond to $|\mathbf{v}|(0, z)$, $|\mathbf{v}|(0.2N_g, z)$, and $|\mathbf{v}|(0.4N_g, z)$, respectively.

applications, it is very important to reduce the device size. Our analytical approach can be very useful from this point of view in that it can determine how far we can reduce the grating size while retaining the required characteristics.

In summary, we have developed a general analytical approach to investigate the slow light effect of the Rayleigh anomaly on diffraction gratings with both infinite and finite sizes. Our study shows that the Rayleigh anomaly can slow down the group velocities of the transmitted light over a very long effective range, but the effect will diminish as the size of the grating shrinks. This phenomenon suggests a new mechanism to improve the light matter interaction that can enhance long-range optical sensing and photodetection.

Funding. National Science Foundation, Directorate for Engineering (ENG) (1342318); National Institutes of Health (NIH) (9R42ES024023).

REFERENCES

1. J. Goodman, *Introduction to Fourier Optics*, 2nd ed. (McGraw-Hill, 1996).
2. R. W. Wood, Phys. Rev. **48**, 928 (1935).
3. J. W. S. Rayleigh, Philos. Mag. **14**(79), 60 (1907).
4. U. Fano, J. Opt. Soc. Am. **31**, 213 (1941).
5. R. C. McPhedran and D. Maystre, Opt. Acta **21**, 413 (1974).
6. M. Sarrazin, J.-P. Vigneron, and J.-M. Vigoureux, Phys. Rev. B **67**, 085415 (2003).
7. J. M. Steele, C. E. Moran, A. Lee, C. M. Aguirre, and N. J. Halas, Phys. Rev. B **68**, 205103 (2003).
8. A. Christ, T. Zentgraf, J. Kuhl, S. G. Tikhodeev, N. A. Gippius, and H. Giessen, Phys. Rev. B **70**, 125113 (2004).
9. J. M. McMahon, J. Henzie, T. W. Odom, G. C. Schatz, and S. K. Gray, Opt. Express **15**, 18119 (2007).
10. H. Gao, J. M. McMahon, M. H. Lee, J. Henzie, S. K. Gray, G. C. Schatz, and T. W. Odom, Opt. Express **17**, 2334 (2009).
11. Y.-W. Jiang, L. D.-C. Tzuang, Y.-H. Ye, Y.-T. Wu, M.-W. Tsai, C.-Y. Chen, and S.-C. Lee, Opt. Express **17**, 2631 (2009).
12. C.-Y. Lin, X. Wang, S. Chakravarty, B. S. Lee, W. Lai, J. Luo, A. K.-Y. Jen, and R. T. Chen, Appl. Phys. Lett. **97**, 093304 (2010).
13. Q. Gan, Z. Fu, Y. J. Ding, and F. J. Bartoli, Phys. Rev. Lett. **100**, 256803 (2008).
14. B. Luk'yanchuk, N. I. Zheludev, S. A. Maier, N. J. Halas, P. Nordlander, H. Giessen, and C. T. Chong, Nat. Mater. **9**, 707 (2010).
15. F. Lopes-Tejeira, R. Paniagua-Dominguez, R. Rodriguez-Oliveros, and J. A. Sanchez-Jil, New J. Phys. **14**, 023035 (2012).
16. J. N. Anker, W. P. Hall, O. Lyandres, N. C. Shah, J. Zhao, and R. P. Van Duyne, Nat. Mater. **7**, 442 (2008).
17. Y. Gao, Z. Xin, B. Zeng, Q. Gan, X. Cheng, and F. J. Bartoli, Lab Chip **13**, 4755 (2013).
18. B. Zeng, Y. Gao, and F. J. Bartoli, Nanoscale **7**, 166 (2015).
19. P. N. Stavrinou and L. Solymar, Opt. Commun. **206**, 217 (2002).
20. M. Born and E. Wolf, *Principles of Optics*, 7th ed. (Cambridge University, 1999).
21. L. J. F. Broer, Appl. Sci. Res. **A2**, 329 (1951).
22. M. A. Biot, Phys. Rev. **105**, 1129 (1957).
23. P. Y. Chen, R. C. McPhedran, C. M. de Sterke, C. G. Poulton, A. A. Asatryan, L. C. Botten, and M. J. Steel, Phys. Rev. A **82**, 053825 (2010).
24. E. Popov, L. Tsonev, and D. MayStre, J. Mod. Opt. **37**, 367 (1990).
25. A. A. Rizvi and C. H. Papas, Prog. Electromag. Res. **29**, 261 (2000).
26. Y. Brûlé, G. Demésy, B. Gralak, and E. Popov, Opt. Express **23**, 9167 (2015).
27. D. M. Natarov, V. O. Byelobrov, R. Sauleau, T. M. Benson, and A. I. Nosich, Opt. Express **19**, 22176 (2011).
28. N. P. Stognii and N. K. Sakhnenko, IEEE J. Sel. Top. Quantum Electron. **19**, 4602207 (2013).